Lesion Enhancement in Radio-Frequency Spoiled Gradient-Echo Imaging: Theory, Experimental Evaluation, and Clinical Implications

Scott Rand,[1] Kenneth R. Maravilla,[1,2] and Udo Schmiedl[1]

PURPOSE: To investigate the lesser lesion conspicuity after gadolinium contrast infusion with radio-frequency spoiled gradient-echo (SPGR) sequences relative to conventional T1-weighted spin-echo techniques. **METHODS:** The influences of repetition time, echo time, and flip angle on spin-echo and SPGR signal were studied with mathematical modeling of the image signal amplitude for concentrations of gadopentetate dimeglumine solute from 0 to 10 mM. Predictions of signal strength were verified in vitro by imaging of a doped water phantom. The effects of standard (0.1 mmol/kg) and high-dose (0.3 mmol/kg) gadoteridol on spin-echo and SPGR images were also investigated in three patients. **RESULTS:** The measured amplitude of undoped water and the rate of increase of doped water signal with increasing gadopentetate concentration (slope) for spin-echo 600/11/1/90° (repetition time/echo time/excitations/flip angle) and SPGR (600/11/190°) were similar and exceeded those of SPGR (35/5/145°). Greater increases in SPGR doped water signal and its slope were produced by increasing TR than by varying echo-time or flip angle. The subjective lesion conspicuity and measured lesion contrast at 0.3 mmol/kg were greater with spin-echo (600/11/1/90°) than with SPGR (35/5/145°) in all three patients; the measured lesion enhancement was similar for both techniques in two patients and decreased for SPGR in the third patient. **CONCLUSIONS:** The phantom studies suggest that the short repetition time of 35 msec, typically used in clinical SPGR imaging, is largely responsible for a reduced signal amplitude and a diminished rate of increase of signal with increasing gadopentetate concentration, relative to spin-echo. Phantom and clinical studies suggest that the dose of paramagnetic agent required to achieve SPGR lesion conspicuity with short repetition time comparable with spin-echo would have to be higher than the dose in current clinical use.

Index terms: Magnetic resonance, contrast enhancement; Magnetic resonance, experimental; Magnetic resonance, gradient-echo; Magnetic resonance, physics

AJNR Am J Neuroradiol 15:27–35, Jan 1994

Radio-frequency spoiled gradient-echo (SPGR) sequences are capable of producing images with tissue contrast and anatomic detail similar to conventional T1-weighted spin-echo (SE) techniques, but with considerably reduced data acquisition times. Previous studies with gradient-echo sequences in which residual transverse coherences were spoiled with gradient pulses reported lesion contrast or enhancement after intravenous gadopentetate both comparable with (1, 2) (Kornmesser W, et al, presented at the annual meeting of the Society of Magnetic Resonance in Medicine, New York, August, 1987) and less than (3) that of spin-echo techniques. However, reduced postgadolinium lesion enhancement has been observed with SPGR relative to SE imaging in recent clinical trials, with the implication of possible undetected or misdiagnosed lesions with SPGR (4) (Augenstein H, Sze G, presented at the annual meeting of the Radiological Society of North America, Chicago, November, 1990).

Although the dependence of image contrast on operator-dependent pulse-sequence parameters has been investigated in detail for SE and gradient-echo techniques (5, 6), the apparent limited effectiveness of gadopentetate in the improve-

Received June 4, 1992; accepted pending revision October 26; revision received March 5, 1993.

[1] Department of Radiology, University of Washington Medical Center, Seattle, WA 98195.

[2] Address correspondence to Kenneth R. Maravilla, MD, Department of Radiology, SB-05, University of Washington Medical Center Seattle, WA 98195.

AJNR 15:27–35, Jan 1994 0195-6108/94/1501-0027

ment of lesion conspicuity in SPGR imaging remains unexplained (Brant-Zawadzki M, presented at the Society of Magnetic Resonance in Medicine Workshop on Contrast-Enhanced Magnetic Resonance, Napa, CA, May, 1991). The present study was undertaken to determine the reasons for the diminished SPGR lesion contrast relative to SE observed after gadolinium administration and to seek means for improved SPGR enhancement.

Methods

This study consisted of a three-part investigation composed of mathematical modelling of signal amplitudes with SE and SPGR, in vitro verification of model predictions with a gadolinium-doped water phantom, and a pilot clinical study of three patients who received standard and high doses of a gadolinium contrast agent.

Prediction of Gadopentetate-Doped Water Signal Amplitude

Theoretical expressions of signal amplitude for the SE and SPGR pulse sequences are listed in the Appendix. Measured water solvent longitudinal (T1) and transverse (T2) relaxation times and longitudinal (R1) and transverse (R2) relaxivities of gadopentetate dimeglumine (Gd-DTPA) (Magnevist, Berlex, Cedar Knolls, NJ) were substituted into these expressions to predict (calculate) SE and SPGR signal amplitudes as a function of gadopentetate concentration (7). The effects of intravoxel incoherent dephasing such as susceptibility artifacts were neglected in the SPGR predictions, and T2* was set equal to T2. Simulations were calculated and plotted on a Macintosh II computer (Apple, Cupertino, CA) using the symbolic mathematics program Mathematica (Wolfram Research, Champaign, IL).

Standard SE images were obtained to measure T1 relaxation times of the phantom. The receiver and transmitter amplification gains were fixed, echo time (TE) was fixed at 20 msec, and repetition time (TR) was varied. Eight TR values of 150, 300, 600, 900, 1200, 1800, 2400, and 4800 msec were used to measure T1 values ranging from 133 to 2382 msec for gadopentetate concentrations up to 1 mM. Five TR values of 50, 67, 83, 100, and 150 msec were used to measure T1 values ranging from 20 to 85 msec for gadopentetate concentrations from 2 to 10 mM. For each gadopentetate concentration and TR value, the signal amplitude was defined as the average value within a region of interest cursor placed over the appropriate centrifuge tube. Measured signal amplitudes as a function of time (TR) were fit to the rising exponential

$$S = N(T2) * (1 - (1 + FR) * \exp[-TR/T1])$$

to solve for pseudo-spin density (N(T2)), flip angle ($\alpha°$;FR = $-\cos(\alpha°)$), and longitudinal relaxation time (T1). This iterative three-parameter curve-fitting program was provided with General Electric software available on the operator's console.

Similarly, standard SE images with fixed receiver and transmitter gains, a fixed TR of 4800 msec, and four TE values of 20, 40, 60, and 80 msec were used to measure transverse relaxation times of the phantom. Measured signal amplitudes as a function of time (TE) were fit to the decaying exponential

$$S = N(T1) * \exp[-TE/T2]$$

to solve for pseudo-spin density (N(T1)) and transverse relaxation time (T2). This iterative two-parameter technique was also provided with General Electric software. Longitudinal (R1) and transverse (R2) relaxivities (1/(mM sec)) were computed with linear least-squares fits to the Solomon-Bloembergen equations listed in the Appendix (8).

Measurement of Gadopentetate-Doped Water Signal Amplitude

All imaging studies were conducted on a General Electric 1.5T Signa system (General Electric, Milwaukee, WI). The phantom consisted of an array of plastic centrifuge tubes filled with deionized, distilled water doped with graded concentrations of gadopentetate. Three serial dilution batches were prepared with the following concentrations: 0.00100 to 10.0 mM Gd-DTPA in multiplicative increments of 1.00×10^{-3}, 1.00×10^{-2}, 1.00×10^{-1}, 1.00, and 1.00×10^{1} mM; 0.100 to 1.00 mM Gd-DTPA in linear (arithmetic) increments of 0.100 mM; and 1.00 to 10.0 mM Gd-DTPA, in linear (arithmetic) increments of 1.00 mM. Reference tubes containing undoped water were also included.

Single section images of the phantom were obtained with the SE and SPGR pulse sequences. A 24-cm field of view, 5-mm section thickness, 256 × 192 matrix, and a single data collection (1 excitation) were used for both techniques. Averages and standard deviations of region of interest signal amplitudes from samples within two or three nominally identical images were obtained for each combination of TR, TE, excitations, and flip angle. Measured signal amplitudes for SE 600/11/1/90° (TR/TE/excitations/flip angle), SPGR 600/11/1/90°, and SPGR 35/5/145° were compared directly, without normalization, because the receiver amplification gain was identical and the transmitter gain was within 0.5 dB for each pulse sequence. Additional sets of SPGR images with fixed receiver and transmitter gains were produced in which either TR, TE, or flip angle varied incrementally.

Pilot Clinical Studies

Multisection clinical SE and SPGR images were obtained in three patients who were participating in a phase III clinical trial investigating the effectiveness of standard versus high doses of a new magnetic resonance (MR) contrast agent, gadoteridol (ProHance, Squibb, Princeton, NJ). Images were obtained before and after the intravenous injection of graded doses of 0.1 and 0.2 mmol/kg that yielded a cumulative dose of 0.3 mmol/kg. SPGR scans were ob-

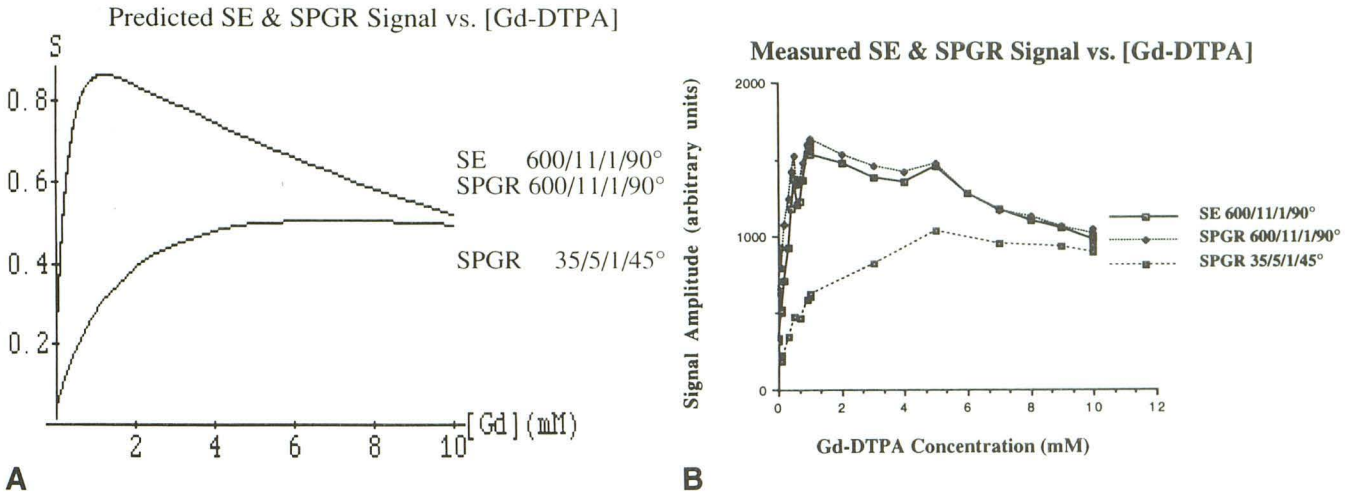

Fig. 1. *A*, Predicted signal amplitudes, S (arbitrary units), versus Gd-DTPA concentration (Gd) (mM), for the SE and SPGR pulse sequences as per equations 1 through 3. The top curve represents the SE 600/11/1/90° and SPGR 600/11/1/90° sequences, which overlap; the bottom curve represents SPGR 35/5/1/45°.

B, Measured image signal amplitudes versus Gd-DTPA concentration of a doped water phantom. Sequence parameters corresponded to those of Figure 1*A*.

tained within 10 minutes of the SE sequence to which they were compared.

The in vitro relaxivities of gadoteridol and gadopentetate are nearly identical [9]. A 20-cm field of view, a 256 × 128 matrix, and a 2.5-mm intersection gap were used. A single data collection (excitation) was employed with SE, whereas two were used with SPGR. Flow compensation gradients were applied to the SPGR sequence to reduce flow artifacts for TE greater than 10 msec. Other imaging parameters were identical to those of the phantom study above. The lesion signal amplitude, contrast, and relative enhancement for SE 600/12/1/90° images were compared with SPGR at 35/5/2/45°. The receiver gain was fixed and the transmitter gain was within 0.7 dB for each sequence, obviating the need for normalization. The 10-minute interval between serial SE scans after gadoteridol injection prescribed in the phase III trial was too short to allow a comparison between SE 600/12/1/90° and SPGR 600/12/1/90°.

Relative lesion-to-background image contrast, Cn, was defined as

$$Cn = (S_L - S_B) / S_B$$

where S_L and S_B represent the average signal amplitude within a region of interest cursor placed over the lesion, and an area of adjacent brain parenchyma (background), respectively. Relative lesion enhancement, E, was defined as the difference between the pre- and postgadoteridol infusion lesion signal amplitudes divided by the pregadoteridol lesion signal strength:

$$E = (S_{Lpost} - S_{Lpre}) / S_{Lpre}$$

Results

Prediction and Measurement of Doped Water Signal Amplitude

The in vitro longitudinal and transverse relaxivities of gadopentetate of 4.85 and 5.46 (1/(mM sec)), respectively, measured at 64 MHz, were consistent with published values measured at 20 MHz of 4.52 and 5.66 (1/(mM sec)), respectively (10, 11). The correlation coefficients of the linear least-squares regression curves for R1 and R2 were 0.98 and 0.99, respectively. Standard deviations of two or three region of interest measurements of signal amplitudes (measurement errors) were all less than 4.8% of the mean values, and typically they were less than 1%. The measurement errors for SE 600/11/1/90°, SPGR 600/11/1/90°, and SPGR 35/5/1/45° were too small to be resolved as "error bars" on the curves in Figure 1*B*; error bars on subsequent Figures 2*B*, 3*B*, and 4*B* were similarly omitted.

The computer-generated predictions of SE and SPGR signal amplitudes as a function of gadolinium concentration (Fig 1A) were indistinguishable when obtained with identical parameters of 600/11/90° that correspond to standard clinical settings for a T1-weighted SE sequence. At low gadopentetate concentrations up to approximately 2.0 mM, including the initial ascending parts of the curves, the measured SPGR 600/11/1/90° signal exceeded that of the SE 600/11/1/90° sequence (Fig. 1*B*). This difference was most pronounced with the undoped water, S_d (the subscript *d* for undoped solute is retained from the spectroscopic literature). This observation was reproduced in subsequent experiments on a different General Electric 1.5-T Signa system, with a second phantom that was made with the same materials and immersed in a tapwater bath to reduce susceptibility effects.

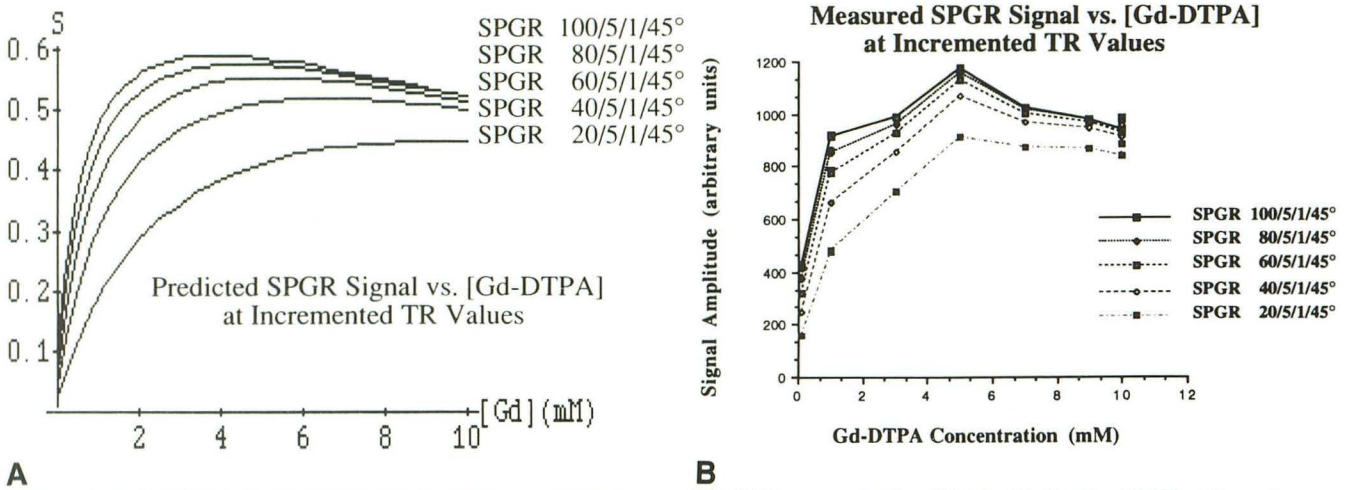

Fig. 2. *A*, Predicted signal amplitudes, S (arbitrary units), versus Gd-DTPA concentration (Gd) (mM), for the SPGR pulse sequence as per equations 1 through 3. TE and flip angle were fixed at 5 msec and 45°, respectively. TR varied from 20 msec in the bottom curve to 100 msec in the top curve by increments of 20 msec.

B, Measured image signal amplitudes versus Gd-DTPA concentration of a doped water phantom. Sequence parameters corresponded to those of *A*.

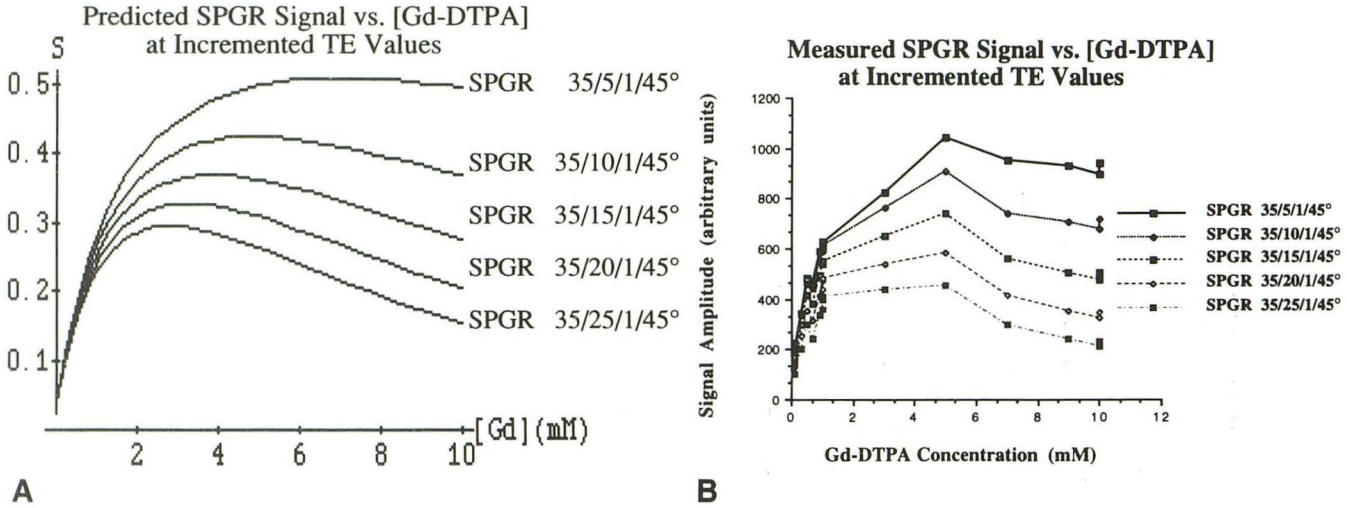

Fig. 3. *A*, Predicted signal amplitudes, S (arbitrary units), versus Gd-DTPA concentration (Gd) (mM), for the SPGR pulse sequence as per equations 1 through 3. TR and α were fixed at 35 msec and 45°, respectively. TE varied from 5 msec in the top curve to 25 msec in the bottom curve by increments of 5 msec.

B, Measured image signal amplitudes versus Gd-DTPA concentration of a doped water phantom. Sequence parameters corresponded to those of Figure 3*A*.

A notch in the initial ascending portion of all three curves in Figure 1*B* at approximately 0.7 mM and a peak at the 5.0 mM sample in Figure 1*B* were considered artifacts likely caused by dilution errors, because they were not reproduced in subsequent experiments with the second phantom in a different 1.5-T system. A peak at the 5.0 nM sample in Figures 2*B*, 3*B*, and 4*B* and a similar notch in the ascending portion of Figure 3*B* at approximately 0.7 nM were attributed to the same artifacts as in Figure 1*B*; time and financial constraints precluded repetition of all of the in vitro experiments. Subtle differences in measured signal amplitudes between the three separate gadopentetate dilution batches (of the first phantom) at nominal concentrations of 0.1, 1.0, and 10.0 mM mirrored subtle differences in the measured T1 and T2 lifetimes. These discrepancies were ascribed to small differences in actual gadopentetate concentration (dilution errors).

For "T1-weighted" SPGR parameters of 35/5/1/45°, both the slope of the initial ascending portions of the theoretical (Fig. 1*A*) and measured (Fig 1*B*) curves and the maximum signal intensity were considerably reduced relative to SE and SPGR at 600/11/1/90°. The gadopentetate concentration at which maximal signal was achieved progressively increased from 1.5 mM for SE and

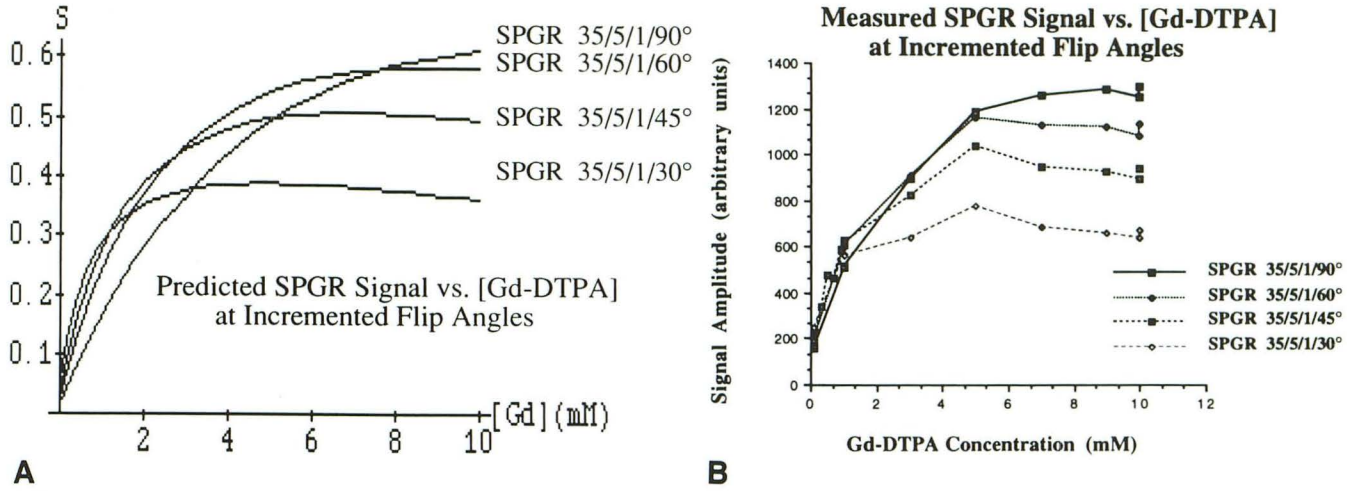

Fig. 4. *A*, Predicted signal amplitudes, S (arbitrary units), versus Gd-DTPA concentration (Gd) (mM), for the SPGR pulse sequence as per equations 1 through 3. TR and TE were fixed at 35 and 5 msec, respectively. Flip angle equaled 90°, 60°, 45°, and 30°, running from the top curve to the bottom curve at the 10 mM concentration.

B, Measured image signal amplitudes versus Gd-DTPA concentration of a doped water phantom. Sequence parameters corresponded to those of Figure 4*A*.

SPGR at 600/11/1/90° to approximately 7 mM for SPGR 35/5/1/45° (neglecting the artifact at 5.0 mM).

As the TR of the SPGR sequence was progressively lengthened from 20 to 100 msec, both the slope of the signal intensity curve and its maximum increased, whereas the gadopentetate concentration required to achieve maximal signal decreased (Figs 2*A* and 2*B*). As TE was increased for the short-TR SPGR sequence, both the maximal signal amplitude and the concentration of gadopentetate required to reach the maximum decreased. The initial slope of the curve was not significantly affected (Figs 3*A* and 3*B*). Finally, as the flip angle was increased for the short-TR sequence from 30° to 90°, the initial slope of the curve decreased, while both the maximum signal and the gadopentetate concentration at which the maximum signal was achieved increased (Figs 4*A* and 4*B*).

Pilot Clinical Studies

The preinjection SE 600/11/1/90° lesion signal strength exceeded that of the SPGR 35/5/2/45° technique in all three patients. This was analogous to phantom results in Figure 1 for the undoped water (gadopentetate concentration of zero). Lesion signal increased with increasing gadoteridol dose for both the SE and SPGR sequences in all three patients. The rate of increase (slope) of the SE 600/11/1/90° signal with increasing dose (up to 0.3 mmol/kg) exceeded that of the SPGR 35/5/2/45° sequence, analogous to the phantom results in Figure 1 within the 0.0 to 1.5 mM Gd-DTPA concentration range.

SE 600/11/1/90° and SPGR 35/5/2/45° images of a representative patient after 0.1 mmol/kg gadoteridol are presented in Figure 5. Lesion signal strength, relative lesion contrast, Cn, and relative lesion enhancement, E, for this patient are presented as a function of gadoteridol dose in Figures 6*A* and 6*B*. The increase in lesion signal with SPGR 35/5/2/45° at a dose of 0.3 mmol/kg relative to the preinjection image resembled the increase in lesion signal observed with SE 600/11/1/90° at 0.1 mmol/kg.

Subjective conspicuity of the enhancing lesions after 0.3 mmol/kg gadoteridol with SE 600/11/1/90° exceeded that with SPGR 35/5/2/45° in all three patients. This correlated well with measurements of relative lesion contrast (Table 1). Measured lesion enhancement (Table 1), however, was very similar for both techniques in two of the three patients (patients 1 and 3), but was decreased in the third patient (patient 2).

Discussion

Unlike normal and pathologic tissues, the behavior of MR signal from bulk water within homogeneous solutions of paramagnetic species is well understood (7). Our comparison of SE and SPGR in vitro made the following implicit assumptions. The application of equations 1 and 2 in the Appendix, derived in the context of MR *spectroscopy*, to *imaging* assumed that the section selection profiles were rectangular and that

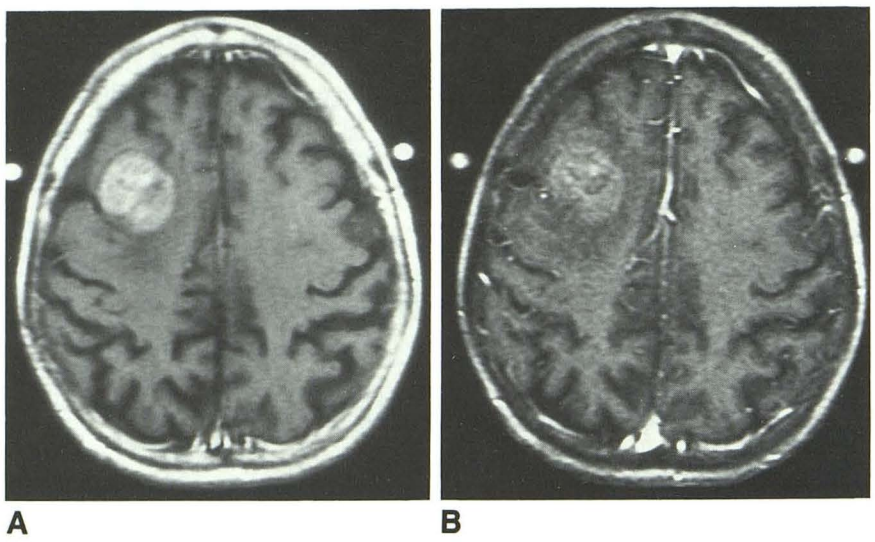

Fig. 5. *A*, Patient with a right frontal metastasis obtained with the SE 600/11/1/1 90° sequence immediately after infusion of 0.1 mmol/kg gatoteridol.

B, Image performed with the SPGR 35/5/2/45° sequence immediately after Figure 5*A* was obtained.

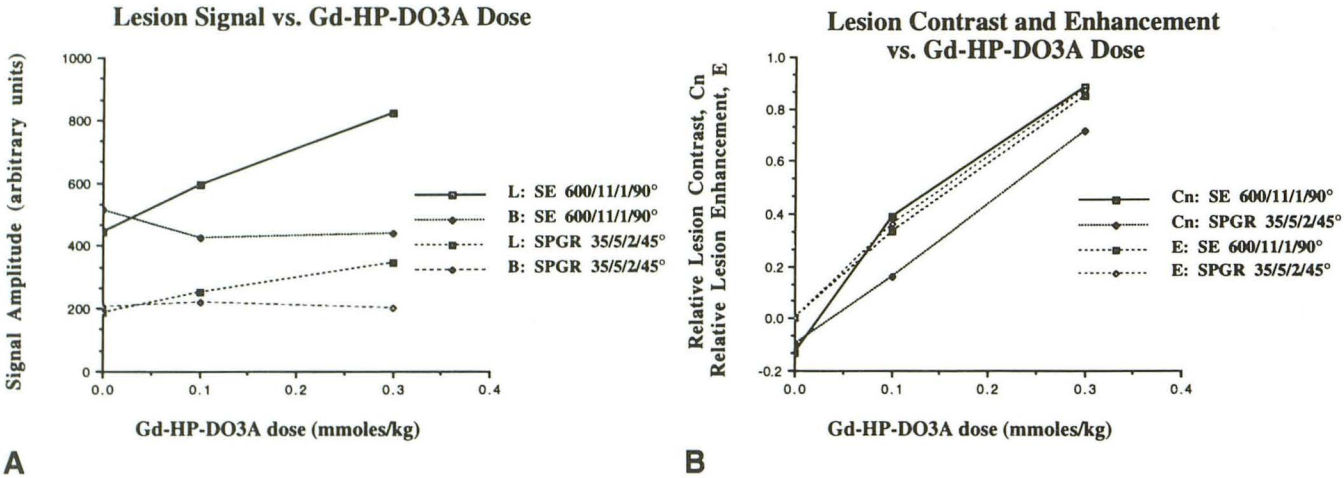

Fig. 6. *A*, Measured signal amplitudes versus gatoteridol (Gd-HP-DO3A) dose of SE and SPGR images corresponding to the same axial section in a patient with a right frontal metastasis, seen in Figure 5. *L* refers to a lesion and *B* refers to the adjacent brain parenchyma (background). The increase in lesion signal with SPGR 35/5/45° at a dose of 0.3 mmol/kg relative to the preinjection image resembles the increase in lesion signal observed with SE 600/11/1/90° at 0.1 mmol/kg.

B, Measured relative lesion-to-background image contrast, Cn, and relative lesion enhancement, E, versus gatoteridol (Gd-HP-DO3A) dose. SE and SPGR images correspond to the axial section in Figure 6*A*. Although the measured lesion contrast with SE 600/11/1/90° exceeds that with SPGR 35/5/2/45° at low (0.1 mmol/kg) and high (0.3 mmol/kg) Gd-HP-DO3A doses, the measured lesion enhancements are similar.

TABLE 1: Lesion signal amplitude, contrast, and enhancement in three patients after 0.3 mmol/kg intravenous gatoteridol

Patient	SE 600/11/1/90°			SPGR 35/5/2/45°		
	S_L[a]	Cn[b]	E[c]	S_L	Cn	E
1	821.84	0.88	0.85	347.29	0.72	0.87
2	678.34	0.96	0.91	313.55	0.63	0.66
3	692.94	0.57	0.84	290.74	0.48	0.88

[a] Lesion signal amplitude, S_L, in arbitrary units.

[b] Relative lesion-to-background contrast, $Cn = (S_L - S_B)/S_B$, where the subscripts *L* and *B* represent the lesion and adjacent brain (background), respectively.

[c] Relative lesion enhancement, $E = (S_{Lpost} - S_{Lpre})/S_{Lpre}$, where the subscripts *pre* and *post* refer to the gatoteridol injection.

the radiofrequency fields were spatially uniform (12). Although local susceptibility effects with gradient-echo sequences are extremely important clinically for air-tissue interfaces, hemosiderin, melanin, etc, susceptibility effects were neglected in the phantom studies. Unlike dysprosium and other "chemical shift reagents," the primary paramagnetic effect of gadolinium ions in vitro is to shorten T1 and T2 lifetimes (broaden spectral lines) rather than to shift the spectral lines. Local perturbations of the magnetic field caused by gadopentetate have been reflected in a small measured upfield Larmor frequency shift of 0.25 ppm at 80 MHz for a concentration of 5 mM (13).

The empirical observation that SPGR 600/11/1/90° signal exceeded SE 600/11/1/90° at low gadopentetate concentration suggests that susceptibility effects in vitro were minor for TE < 12 msec.

The kinetics of gadoteridol administration were assumed constant in the clinical studies, neglecting any possible delayed enhancement effects (Augenstein H, Sze G, presented at the annual meeting of the Radiological Society of North America, Chicago, November, 1990). Finally, the analysis did not address differences in other factors that can influence image interpretation such as fidelity and distortion (patient motion, field inhomogeneity, cerebrospinal fluid or blood flow, and susceptibility artifacts), spatial resolution (point-spread function), noise, and the arbitrary choice of window and level settings for image display.

Prediction and Measurement of Doped Water Signal

The reproducible small increase in SPGR 600/11/1/90° signal over SE 600/11/1/90° at low gadopentetate concentrations (Fig 1*B*) was not supported by the mathematical model (Fig 1*A*). The cause of this observation is unclear because local inhomogeneities in the main magnetic field, susceptibility effects, or imperfections in gradient field reversal would be expected to diminish SPGR 600/11/1/90° signal relative to SE 600/11/1/90°. Although the section-selective 90° excitation pulses for SE and SPGR were nominally identical (programmed with the same computer code), this signal discrepancy may relate to the selective 180° refocusing radiofrequency pulse used with SE but not with SPGR. (The influence of imperfections in the 180° pulse are not incorporated into the Bloch equation solutions in the Appendix.) Saturation from imperfections in the nominal 180° flip angle, if any, would be most evident for long T1 species (low gadopentetate concentrations). Any imperfections in phase coherence (phase errors) across the section immediately after the 180° pulse would be most evident for long T2 species (low gadopentetate concentrations) and long TE values. Any narrowing or misregistration of the 180° section profile relative to the 90° section would be expected to refocus the spin echo incompletely and produce a diminished SE signal that was relatively independent of gadopentetate concentration.

At small gadopentetate concentrations in which the T1 effects dominate, the T2 or T2* effects can be ignored in vitro (7). Equations 1 and 2 can then be approximated by the same quantity,

$$S_{SE} \sim S_{SPGR} \sim S = 1 - \exp[-TR/T1]$$

This rising exponential function represents the partial saturation effects within the initial ascending portion of the signal intensity curves in Figures 1 through 4.

A greater percentage of protons are saturated in the longitudinal steady state for a TR of 35 msec than for a TR of 600 msec, regardless of the type of echo recorded. Thus, more efficient longitudinal relaxation through a greater gadopentetate concentration is required with a very short TR SPGR than with SPGR or SE using longer TR, to achieve a given percentage of protons at equilibrium immediately before an excitation pulse in each sequence. The SPGR 35/5/1/45° sequence produced a signal maximum approximately equal to 75% of the maximum for SE 600/11/1/90°, but at a fivefold increase in gadopentetate concentration from 1.5 to 7 mM (Fig 1).

For a fixed *small* gadopentetate concentration, *short* TE, and a 90° *flip*, increasing TR for either SE or SPGR yields a greater signal, according to the above equation. Similarly, as TR lengthens for SPGR with a 45° flip (Fig 2), a reduced percentage of saturated protons in the steady state is responsible for a greater signal strength of undoped water, a steeper initial rate of change with increasing gadopentetate concentration, and a larger signal maximum. This finding is consistent with a reduced postgadopentetate lesion conspicuity observed with a fast low-angle shot 250/12/2/90° as compared with SE 500/17/2/90°, where the TR values differ by a factor of two (4).

The influence of flip angle on short TR SPGR signal strength in equation 2 in the Appendix is mathematically more complicated than the partial saturation effects described above. The flip angle that optimizes signal strength (Ernst angle) is less than 90° when the repetition time is reduced such that TR < T1 because saturation of the longitudinal magnetization becomes significant in the steady state (14). Thus, at gadopentetate concentrations less than 2 mM, in which TR < T1, a 30° flip produced a slightly greater signal strength of undoped water, and a greater initial rate of signal rise, than did a 90° flip (Fig 4).

Pilot Clinical Studies

Phantom experiments with gadoteridol would be expected to mimic those of gadopentetate above, given the similarity of their in vitro relaxivities (9). Obviously, the extrapolation of phantom study results to the clinical regime is difficult because factors governing paramagnetic agent permeability and kinetics across an abnormal blood brain barrier in intracranial mass lesions are complex. Furthermore, effective paramagnetic agent relaxivities in aqueous solutions (or serum) and tissues may differ or may be measured in different units. However, a linear empiric relationship between in vivo transverse relaxation rate (1/T1) and normal myocardial tissue gadoteridol concentration (mmol/g) analogous to equation 3 has been reported over a limited tissue concentration range and dose in an animal model (Tweedle M, presented at the Society of Magnetic Resonance in Medicine Workshop on Contrast-Enhanced Magnetic Resonance, Napa, CA, May, 1991).

The observed differences in postgadoteridol signal between T1 weighted SE (600/11/1/90°) and T1-weighted short TR SPGR (35/5/1/45°) clinical images were likely related to the different choices of imaging parameters (TR/TE/excitations/α°) rather than to inherent differences in the pulse sequences. These findings are consistent with the observation of comparable postgadopentetate lesion contrast for the SE 400/30/2/90° and fast low-angle shot 315/14/1/90° techniques, where the TR, TE, and flip angle values were more similar (15). (Residual transverse coherences in the fast low-angle shot sequence are destroyed with gradient pulses rather than with radio-frequency spoiling, and thus fast low-angle shot signal amplitudes are approximated with equation 2.) Apart from intravoxel incoherence effects produced by local susceptibility differences (particularly notable with air-tissue interfaces, hemosiderin, etc) and with other factors being equal, the type of echo recorded (spin echo vs gradient echo) may determine the observed object dependent noise, spatial resolution, and artifacts of the image, but not the image contrast.

The trends observed in Figures 5 and 6 and Table 1 are consistent with the phantom studies above. The lesion signal amplitude, relative lesion contrast, Cn, and relative lesion enhancement, E, increased with rising gadoteridol dose over the range of 0 to 0.3 mmol/kg. This dose range is analogous to the low gadopentetate concentration regime of 0 to 1.5 mM in the phantom studies, where T1 effects dominate over T2 or T2* effects.

Although lesion *enhancement* is frequently reported in the literature, lesion *contrast* is a better measure of lesion *visibility* or *conspicuity* in the evaluation of postinjection images. Lesion contrast and enhancement would be similar to the extent that the preinjection signal strength of the lesion is isointense with nonenhancing adjacent brain parenchyma. However, because pathologic lesions are commonly hypointense to brain parenchyma, as in Figure 6*A*, the measured postinjection enhancement may overstate lesion conspicuity when the contrast agent increases the lesion signal strength to be nearly isointense to, but not significantly greater than, adjacent brain parenchyma.

For example, after 0.1 mmol/kg gadoteridol, the lesion illustrated in Figure 5 is more conspicuous with SE 600/11/1/90° than with SPGR 35/5/2/45° and the measured lesion contrast is also greater with SE 600/11/1/90° (Figure 6*B*). However, the measured lesion enhancements are similar for both SE 600/11/1/90° and SPGR 35/5/2/45° at low (0.1 mmol/kg) and high (0.3 mmol/kg) gadoteridol doses (Figure 6*B*, Table 1). This discrepancy between lesion contrast (conspicuity) and measured enhancement may be particularly relevant to SPGR as one cause for apparent decreased lesion conspicuity after gadolinium when compared with T1-weighted SE imaging.

Conclusion

Results from the current study indicate that the short TR of the T1-weighted SPGR sequence is largely responsible for the diminished postinjection lesion contrast observed with SPGR 35/5/2/45° relative to SE 600/11/1/90°. Mathematical modelling and phantom imaging suggest that differences in TE and flip angle make minor contributions to the observed differences in lesion contrast with each technique. Phantom imaging suggests that clinical SPGR lesion enhancement may be most improved by increasing TR, at the obvious expense of increased data acquisition time. The dose of paramagnetic contrast media required to achieve short TR SPGR lesion contrast comparable with SE (if possible in vivo) may have to be higher than the current clinical dose. Alternatively, chelates with relaxivities greater than that of gadopentetate, but administered at the current clinical dose, may improve the effi-

cacy of contrast-enhanced short TR SPGR imaging. Finally, our pilot clinical studies suggest that the lesser lesion conspicuity after gadopentetate with SPGR compared with SE may be related, in some cases, to poor lesion-to-background contrast despite nearly equal absolute lesion enhancement.

Appendix

Theoretic expressions of signal amplitude for the SE and SPGR pulse sequences are listed below in equations 1 and 2, respectively (12, 16–19):

$$S_{SE} = S_0\left[1 + \exp\left\{\frac{-TR}{T_1}\right\} - 2\exp\left\{\frac{-(TR - TE/2)}{T_1}\right\}\right]\exp\left\{\frac{-TE}{T_2}\right\} \quad 1$$

$$S_{SPGR} = \frac{S_0\left[1 - \exp\left\{\frac{-TR}{T_1}\right\}\right]\sin\alpha\exp\left\{\frac{-TE}{T_2^*}\right\}}{\left[1 - \cos\alpha\exp\left\{\frac{-TR}{T_1}\right\}\right]} \quad 2$$

where S_0 represents the inherent sensitivity of the instrument that is arbitrarily set to unity, and α represents the flip angle.

Measured in vitro longitudinal (R1) and transverse (R2) relaxivities (1/(mM sec)) were computed with linear least-squares fits to the Solomon-Bloembergen equations (8):

$$1/T1_{eff} = 1/T1_d + (R1 * C) \quad 3$$

$$1/T2_{eff} = 1/T2_d + (R2 * C)$$

where the subscripts *eff* and *d* refer to lifetimes with and without gadopentetate (the *d* subscript for undoped solute is retained from the spectroscopic literature), and C refers to gadopentetate concentration (mM).

Acknowledgments

We are grateful to Pamela Tazioli, RT, and the technical staff of the clinical MRI facility at the University of Washington Medical Center for their assistance in acquiring MR images.

References

1. Runge V. *Enhanced magnetic resonance imaging.* St Louis: C. V. Mosby, 1989:43
2. Runge V, Gelblum D, Wood M. 3-D imaging of the CNS. *Neuroradiology* 1990;32:356–366
3. Laniado M, Kornmesser W, Nagel R, et al. *Spin-echo, inversion-recovery, and fast imaging sequences with Gd-DTPA-enhanced magnetic resonance imaging of renal tumors.* San Diego, CA: Excerpta Medica, 1986:162–165
4. Cherryman G, Golfieri R. Comparison of spin echo T1-weighted and FLASH 90 gadolinium-enhanced magnetic resonance imaging in the detection of cerebral metastases. *Br J Radiol* 1990;63:712–715
5. Stadnik T, Luypaert R, Neirynck E, Osteaux M. Optimization of sequence parameters in fast MR imaging of the brain with FLASH. *AJNR: Am J Neuroradiol* 1989;10:357–362
6. Buxton R, Edelman R, Rosen B, Wismer G, Brady T. Contrast in rapid MR imaging: T1- and T2-weighted imaging. *J Comput Assis Tomogr* 1987;11:7–16
7. Gadian D, Payne J, Bryant D, Young I, Carr D, Bydder G. Gadolinium-DTPA as a contrast agent in MR imaging: theoretical projections and practical observations. *J Comput Assis Tomogr* 1985;9:242–251
8. Davis P, Parker D, Nelson J, Gillen J, Runge V. Interactions of paramagnetic contrast agents and the spin echo pulse sequence. *Invest Radiol* 1988;23:381–388
9. Runge V, Daphna Y, Pacetti M, Carolan F, Heard G. Gd-HP-D03A in clinical MR imaging of the brain. *Radiology* 1990;177:393–400
10. Weinmann H, Brasch R, Press W, Wesby G. Characteristics of gadolinium-DTPA complex: a potential NMR contrast agent. *AJR: Am J Radiol* 1984;142:619–624
11. Lauffer R. Paramagnetic metal complexes as water proton relaxation agents for NMR imaging: theory and design. *Chem Rev* 1987;87:901–927
12. Edelstein W, Bottomley P, Hart H, Smith L. Signal, noise, and contrast in nuclear magnetic resonance (NMR) imaging. *J Comput Assist Tomogr* 1983;7:391–401
13. Wesby G. Paramagnetic shift probes for myocardial nuclear magnetic resonance spectroscopy. Excerpta Medica, 1986
14. Ernst R, Anderson W. Application of Fourier transform spectroscopy to magnetic resonance. *Rev Sci Instr* 1966;37:93–101
15. Schorner W, Sander B, Henkes H, Heim T, Lanksch W, Felix R. Multiple slice FLASH imaging: an improved pulse sequence for contrast enhanced MR brain studies. *Neuroradiology* 1990;32:474–480
16. Wehrli F, MacFall J, Shutts D, Breger R, Herfkens R. Mechanisms of contrast in NMR imaging. *J Comput Assist Tomogr* 1984;8:369–380
17. van der Meullen P, Groen J, Cuppen J. Very fast MR imaging by field echoes and small angle excitation. *Magn Reson Imag* 1985;3:297–299
18. Crawley A, Wood M, Henkelman R. Elimination of transverse coherences in FLASH MRI. *Magn Reson Med* 1988;8:248–260
19. Zur Y, Wood M, Neuringer L. Spoiling of transverse magnetization in steady-state sequences. *Magn Reson Med* 1991;21:251–263